Impact of temperature-driven cycling of hydrogen peroxide (H_2O_2) between air and snow on the planetary boundary layer

Manuel A. Hutterli,[1] Joseph R. McConnell,[2] Richard W. Stewart,[3] Hans-Werner Jacobi,[1] and Roger C. Bales[1]

Abstract

Hydrogen peroxide (H_2O_2) contributes to the atmosphere's oxidizing capacity, which determines the lifetime of atmospheric trace species. Measured bidirectional summertime H_2O_2 fluxes from the snowpack at Summit, Greenland, in June 1996 reveal a daytime H_2O_2 release from the surface snow reservoir and a partial redeposition at night. The observations also provide the first direct evidence of a strong net summertime H_2O_2 release from the snowpack, enhancing average boundary layer H_2O_2 concentrations approximately sevenfold and the OH and HO_2 concentrations by 70% and 50%, respectively, relative to that estimated from photochemical modeling in the absence of the snowpack source. The total H_2O_2 release over a 12-day period was of the order of 5×10^{13} molecules m^{-2} s^{-1} and compares well with observed concentration changes in the top snow layer. Photochemical and air-snow interaction modeling indicate that the net snowpack release is driven by temperature-induced uptake and release of H_2O_2 as deposited snow, which is supersaturated with respect to ice-air partitioning, approaches equilibrium. The results show that the physical cycling of H_2O_2 and possibly other volatile species is a key to understanding snowpacks as complex physical-photochemical reactors and has far reaching implications for the interpretation of ice core records as well as for the photochemistry in polar regions and in the vicinity of snowpacks in general.

1. Introduction

Hydrogen peroxide (H_2O_2) is a significant reservoir for the gas phase oxidants OH and HO_2 and is itself a powerful oxidant in the liquid phase. It thus plays a major role in determining the oxidizing capacity of the atmosphere [*Thompson,* 1992]. In the last decade, ice core records of H_2O_2 were established in part to provide a validation tool for global photochemical models investigating changing atmospheric composition and chemistry [*Sigg and Neftel,* 1991; *Thompson,* 1992; *Anklin and Bales,* 1997]. However, the reliability of these records was questioned when it was found that measured atmospheric H_2O_2 concentrations at Summit (72.6° N, 38.5° W, 3200 m elevation) were higher than predicted by gas phase photochemistry alone and that H_2O_2 concentrations in fresh snow were higher than those in equilibrium with the atmosphere, suggesting considerable exchange of H_2O_2 between the snow and atmosphere [*Conklin et al.,* 1993; *Neftel et al.,* 1995; *Fuhrer et al.,* 1996; *McConnell et al.,* 1997]. However, past studies have failed to directly measure H_2O_2 release from the snowpack [*Bales et al.,* 1995a, 1995b; *Fuhrer et al.,* 1996]. Further, there is strong evidence that formaldehyde (HCHO) desorbs from surface snow in response to diurnal and seasonal temperature changes, leading to H_2O_2 production [*Fuhrer et al.,* 1996; *Hutterli et al.,* 1999; *Couch et al.,* 2000]; this would also occur if HCHO was produced by heterogeneous photochemical reactions in the snow [*Fuhrer et al.,* 1996; *Sumner and Shepson,* 1999]. To further complicate the matter, it has recently been speculated that heterogeneous photochemical production of nitrogen oxides (NO_x) in snow might induce H_2O_2 production [*Jones et al.,* 2000; *Honrath et al.,* 2000].

The present study had three goals. The first was to directly determine H_2O_2 fluxes from the snowpack at Summit with continuous gradient measurements and to compare them with independent estimates based on H_2O_2 concentration changes in the near surface snow. The second goal was to test whether the measurements are consistent with temperature-dependent air-ice partitioning alone, using an existing transfer model [*McConnell et al.,* 1998]. The third goal was to investigate the impact of measured H_2O_2 and HCHO fluxes on atmospheric H_2O_2 and HCHO mixing ratios using a photochemical model and to compare the results with the measurements.

2. Methods

The work was carried out at an electrically heated laboratory module situated 400 m SE of the main structures at the Greenland Ice Sheet Project (GISP2) Camp at Summit, Greenland (72.6° N, 38.5° W, 3200 m elevation) from June 4 to 20, 1996. H_2O_2 was continuously monitored in the air, with the instrument intake line mounted on a lift located 4 m upwind of the laboratory. The lift automatically switched the intake line between heights of 0.06 m and 3.5 m above the snow surface every 12 min. The 7 m long 1/4" perfluoroalkoxy (PFA) intake line was insulated and heated to prevent condensation and was tested several times during the field season for H_2O_2 losses and contamination by comparing various intake lines of different lengths. No artifacts were detected. Note that the use of a single intake line instead of one at each height reduces possible artificial concentration gradients due to line losses. On June 20, H_2O_2 was also measured in the firn air in the top few centimeters of the snowpack, by simply sticking the intake line into a small hole in the surface snow that was made with a polytetrafluoroethylene (PTFE) tool.

Gas phase measurements were done according to *Sigg et al.* [1992] by drawing air (~ 1 L min^{-1} (STP)) and pumping H_2O_2 free water (0.4 mL min^{-1}) together into a coil scrubber, resulting in 100% H_2O_2 collection efficiency. Subsequently, the H_2O_2 content in the water was continuously analyzed by fluorescence spectrometry after derivatization with 4-ethylphenol in the presence of peroxidase [*Sigg et al.,* 1992]. However, instead of raising the pH by adding a NaOH solution with a separate channel, the sample-reagent mixture was pumped through a short membrane tubing (Accurel) that was suspended over a 25% NH_3 solution. Calibrations were performed twice a day by running liquid standards through the coil scrubber while it was flushed with H_2O_2-free air, which was generated by pumping ambient air through a MnO_2 column. Those standards were compared with liquid standards measured directly to check for H_2O_2 losses in the coil scrubber. No losses were detected. The detector was kept at 25°C ±1°C. The baseline was determined every hour by measuring H_2O_2-free air through the intake line. Analytical precision, defined as 3 times the signal noise, was 40 pptv and the accuracy better than 20%.

Sets of five surface snow samples were collected daily at various times (Figure 1e). Each set represented a 2-cm-deep "minipit" with a vertical resolu-

Figure 1

tion of 0.5 cm and the top 0.5 cm layer sampled twice. During high winds, drifting snow samples were collected. However, it was not possible to distinguish between pure drifting snow and the fresh snow that apparently fell during those time periods, so that the samples are potentially a mixture of both. Some pure fresh snow samples were also collected in glass bottles using a high density polyethylene funnel (Figure 1e). Shallow firn cores extending down to 4 m were also collected. H_2O_2 and HCHO concentrations in the various snow samples were simultaneously determined according to *Röthlisberger et al.* [2000] in the field within less than a day after sampling. A more detailed description of the sampling procedures, a representative H_2O_2 concentration profile in the firn, and the HCHO results are given by *Hutterli et al.* [1999]. Firn temperatures were measured with a standard digital thermometer (Technotherm 300, $\pm$ 0.3°C).

Meteorological data were obtained from the GISP2 Automatic Weather Station at Summit (http://uwamrc.ssec.wisc.edu/aws/awsproj.html). Air temperatures were measured at 0.5 and 3.0 m, and wind speed and wind direction were measured at 3 m above the snow surface. Ozone was measured as documented previously [*Bales et al.,* 1995b]. Fog observations were made intermittently and thus reflect only a lower limit for the number of actual fog events.

3. Models

Photochemical modeling was conducted using the NASA Goddard Space Flight Center model [*Stewart and Thompson,* 1996] adapted for Summit conditions (72.3°N, 3 km elevation, and mixed layer height of 100 m [*Neftel et al.,* 1995; *Bales et al.,* 1995b]). A simulation of the measured H_2O_2 and HCHO [*Hutterli et al.,* 1999] fluxes was also included in the model. The model fluxes had the same maximum magnitude and diurnal variation as the observations but were assumed to have a sinusoidal form. In a box model, these fluxes (molecules $m^{-2} s^{-1}$) must be converted to sources (molecules $m^{-3} s^{-1}$) and to this end we usually used a mixed layer height of 100 m to determine the appropriate H_2O_2 and HCHO source functions. Such sources scale directly with the assumed mixed layer height and some results for an assumed 200 m value are indicated in the text and figures.

The lateral extent of the model domain is implicit in an assumed mixing time, a parameter used to specify the coupling to the ambient atmosphere [*Stewart et al.,* 1983]. The mixing time is an *e*-folding time that, in absence of chemistry, would tend to equilibrate the computed species in the box with the fixed values in the ambient atmosphere. In the present model the assumed mixing time is 1 year, so the box is nearly isolated. Water vapor is calculated assuming a relative humidity of 80%. Column-integrated ozone amounts and ozone (O_3), carbon monoxide (CO), and methane (CH_4) observations were used at 3-hour intervals to constrain the model chemistry. The values are based on either satellite measurements or measurements at remote sites in the Northern Hemisphere from the National Oceanic and Atmospheric Administration (NOAA) [*GLOBALVIEW-CH4,* 1999] (data are available on www.cmdl.noaa.gov/info/ftpdata.html). Ozone was further verified using the few available measurements at Summit.

The chemical mechanism used in the present mode is similar to that of *Stewart and Thompson* [1996]. Oxidation of ethene has been added as have reactions involving Cl and Br. As explained in the reference, changing the reaction scheme in the model is handled by a preprocessor and does not require any code modification. The added reactions are all from *DeMore et al.* [1997]. To construct the continuity equations, the model uses 113 reactions and photolyses rates among 48 variable species along with specified physical production and loss terms for some species. Photolysis rates are interpolated from table values generated from the model of *Madronich* [1987]. These tables are written as functions of column-integrated ozone amounts and zenith angle. The kinetic data used are mostly taken from *DeMore et al.* [1997] and *Atkinson et al.* [1992]. The reactions are those following the photolyses of O_3 to produce $O(^1D)$ and the subsequent reaction of some of the latter with water vapor to form OH. In addition to methane, oxidation of ethane (C_2H_6) and ethene (C_2H_4) are included in the model. Ethane values are maintained by an assumed constant flux chosen to give nighttime values in the 2-3 ppbv range consistent with the values measured by *Jobson et al.* [1994] during the Polar Sunrise Experiment. Ethene values measured elsewhere may be about a factor of 2 lower [*Poisson et al.,* 2000] and a flux adjusted to give ~1 ppbv nighttime values was used. Both species are substantially oxidized during the Arctic day. The overall odd nitrogen background is maintained by a specified constant NO source and is about 4 pptv (NO_x). Since ozone is constrained by observed values in this model, the effect of varying assumed NO_x source is small relative to that in a model with ozone responsive to NO_x changes. Methyl chlo-

ride (CH_3Cl) and methyl bromide (CH_3Br) are also included in the chemistry to provide a basic source of halogens. CH_3Cl is held fixed at 600 pptv [*Graedel and Keene,* 1995] and CH_3Br at 10 pptv [*Yokouchi et al.,* 2000]. First-order loss of several species to the ice/snow surface is computed using deposition velocities taken from the summary of *Seinfeld and Pandis* [1998].

The numerical methods used in the model have been described by *Stewart* [1993, 1995] and *Stewart and Thompson* [1996]. The model was run in a time-dependent mode constrained by observations. Temperature, column-integrated ozone amount, and concentrations of methane, carbon monoxide, and ozone were used to update the model at 3-hour intervals. Reaction rates and physical source and loss values are updated every 10 min during a simulation to ensure that photolysis rates are computed at reasonable intervals. The model has previously been employed in Monte Carlo studies of modeling uncertainties [*Stewart and Thompson,* 1996] and in studies related to snow-to-firn transfer of H_2O_2 at the South Pole [*McConnell et al.,* 1998].

The transfer model described by *McConnell et al.* [1998] was used to model the exchange of H_2O_2 between the air and the snowpack. The simulation of the uptake and release of H_2O_2 by snow as environmental conditions change is simulated by the one-dimensional advection-dispersion equation and grain-scale spherical diffusion. Both air-snow partitioning of H_2O_2 and diffusion rates in ice are strongly temperature dependent, with coefficients derived from independent laboratory experiments [*Conklin et al.,* 1993]. In addition to temperature, rates of uptake and release are closely related to grain size and firn ventilation.

In the simulations reported here, we used a 100-layer model with layer thicknesses of 0.5 cm. Measured atmospheric concentrations at 3.5 m provided the upper boundary condition. Firn temperatures were modeled using measured air temperatures and diffusion into the snowpack [*Schwander et al.,* 1997]. Comparison with measurements shows that modeled values in the top few centimeters of the snowpack can be off by up to a few degrees on certain days [*Hutterli,* 1999]. This can be explained with uncertainties inherent in air and snow temperature measurements and with the fact that potential radiation effects [*Colbeck,* 1989] are not taken into account in the model. However, measured temperatures in deeper layers are reproduced within less than 0.5°C, indicating that average temperatures also of the top snow layers are accurately described on daily and longer term timescales [*Hutterli,* 1999]. The uncertainties in the temperature model thus do not significantly affect the average flux estimates. However, on shorter timescales they may have contributed to differences between the modeled and measured H_2O_2 firn air concentrations (Table 1).

Table 1

Molecular diffusion within the firn air was parameterized according to *Hutterli et al.* [1999], with typical H_2O_2 diffusivities of the order of 2.2×10^{-5} m^2 s^{-1}. The initial concentration of H_2O_2 in the snowpack was based on surface snow measurements for the top 2 cm and a snowpit profile of concentration from 2 cm to 50 cm depth, sampled in the same area as the surface snow measurements on June 4 [*Hutterli et al.,* 1999]. H_2O_2 was assumed to initially be distributed uniformly within the snow grains. This simplification might have an impact on the modeled fluxes in the first few days. However, it is not expected to influence the total H_2O_2 release because the initial H_2O_2 distribution within the snow grains adapts fast due to the high diffusion rates at the measured temperatures.

4. Results and Discussion

4.1. Atmospheric Measurements

Atmospheric H_2O_2 showed a distinct diurnal cycle closely linked to temperature with hourly H_2O_2 mixing ratios averaging 1.4 ppbv (range 0.09-4.6 ppbv) for both heights (Figure 1a), consistent with prior summertime measurements [*Bales et al.,* 1995b; *Sigg et al.,* 1992]. From June 4 to 16, wind speed was generally below 5 m s^{-1} (Figure 1d), and fog built up during nearly every night, resulting in rime deposition.

During this period, H_2O_2 gradients in the air above the snow showed a distinct diurnal cycle with positive values (uptake) from evening to midnight and negative values (release) during the rest of the day (Figures 2a and 2b). H_2O_2 gradients were generally between ±0.1 ppbv m^{-1} (Figures 1b and 2b), with an average of -0.020 ppbv m^{-1} which is below the detection limits of earlier studies [*Bales et al.,* 1995b]. From June 17 to 21 there was less nighttime cooling, higher daily mean temperatures (Figure 1c) and wind speeds were up to 15 m s^{-1}, resulting in drifting snow and a higher variability and no distinct diurnal cycle in the H_2O_2 gradients (Figures 1a and 1b). The lifetime of H_2O_2 of less than 2 days at Summit in summer and the remoteness of the site limit the potential impact of long-range transport of H_2O_2

Figures 2

on atmospheric concentrations at Summit. However, the meteorological conditions during the period after June 16 indicated more vigorous long range transport (i.e., lower transport times of air masses from potential direct H_2O_2 sources to Summit). A contribution from H_2O_2 enriched air masses to the high concentrations during this period can thus not be excluded.

H_2O_2 fluxes were determined from the gradient measurements and diffusion coefficients calculated based on the Monin-Obukhov similarity theory according to

$$F = -K_{zz}\frac{\partial C}{\partial z} = -\frac{\kappa u_* z}{\phi(z/L)}\frac{\partial C}{\partial z}, \qquad (1)$$

where C is the atmospheric concentration, z is the height, F is the particle flux, K_{zz} is the turbulent diffusion coefficient, κ (set to 0.40) is the von Karman constant, u_* is the friction velocity, and $\phi(z/L)$ is an empirically determined function defining the flux-profile relationship, which is assumed to depend only on the stability parameter z/L, with L the Monin-Obukhov length [*Seinfeld and Pandis,* 1998]. Variable u_* was obtained iteratively following *King et al.* [1996], using the same parameters and integrated ϕ functions that were determined empirically over the Antarctic ice shelf at Halley station for stable and neutral conditions [*King and Anderson,* 1994]. For unstable conditions the ϕ functions proposed by *Högström* [1988] were used. Finally, the fluxes F were obtained by integrating (1) from measurement heights z_1 to z_2 and inserting the observed atmospheric concentrations $C(z_1)$ and $C(z_2)$.

Implicit in the above flux calculations is the assumption of a constant flux at all heights at any given time. For unstable to moderately stable conditions this is justified by the long characteristic times of chemical reactions involving H_2O_2 (lifetime of $\sim$43 hours at Summit in summer) compared to transport time between the measurement heights (seconds to minutes). This also holds for HCHO (lifetime 3.7 hours at Summit in summer) released by the snowpack, which represents a potentially significant radical source increasing H_2O_2 production [*Hutterli et al.,* 1999]. Stable conditions, with K_{zz} values less than 0.1% of those for unstable conditions, do not contribute significantly to the average H_2O_2 flux and can thus be neglected.

Average H_2O_2 fluxes for each hour of the day for the 12-day period between June 4 and 16 are shown in Figure 2c. Nighttime fluxes are lower due to more stable stratification compared to daytime, when temperature gradients show stratification becoming unstable (Figure 2e). Two outliers, when high wind in combination with a very strong negative temperature gradient led to unreasonably high mixing, were removed from the 164 hourly values. Values for K_{zz} ranged from less than 10^{-5} to 0.9 $m^2\,s^{-1}$, with an average of 0.13 $m^2\,s^{-1}$ for the 12-day period (K_{zz} values lower than the typical molecular diffusivity of 2.4×10^{-5} $m^2\,s^{-1}$ for H_2O_2 under Summit conditions were replaced by this value for consistency; however, this had no effect on the flux calculations). The average flux ($\pm$ standard deviation of the mean) during this period was $(4.9\pm0.9)\times10^{13}$ $m^{-2}\,s^{-1}$ ($(6.3\pm1.3)\times10^{13}$ $m^{-2}\,s^{-1}$ including the outliers). Error propagation calculations based on the meteorological data indicate an uncertainty of the average flux of less than a factor of 2.

4.2. Photochemical Model Runs

Without including H_2O_2 and HCHO fluxes from the snowpack, the gas phase photochemical model results predict average summertime mixing ratios of approximately 0.21 and 0.024 ppbv for H_2O_2 and HCHO, respectively for Summit (Figure 3). This is about one seventh and one tenth of the observed 1.4 and 0.23 ppbv [*Hutterli et al.,* 1999], respectively. This inability of gas phase photochemistry to replicate the observed summer high-latitude H_2O_2 and HCHO mixing ratios has been encountered in other model studies [e.g., *Fuhrer et al.,* 1996]. H_2O_2 fluxes in the observed range of 1.5×10^{13} to 5×10^{13} $m^{-2}s^{-1}$ increase the H_2O_2 mixing ratios to 1.3-3.3 ppbv (0.8-1.8 ppbv) and HCHO mixing ratios to 0.039-0.061 ppbv (0.033-0.055 ppbv), respectively, assuming a typical mixing height of 100 m (200 m) for Summit [*Bales et al.,* 1995b]. Inclusion of the reported HCHO flux of 1×10^{13} $m^{-2}\,s^{-1}$ [*Hutterli et al.,* 1999] into the model adds an additional 0.06 ppbv of HCHO and increases H_2O_2 by about 0.1 ppbv (100 m mixing height), consistent with estimates from earlier model simulations [*Hutterli et al.,* 1999]. While modeled H_2O_2 levels fall within the observed range, modeled HCHO concentrations are lower than observed. The combined effect of the H_2O_2 and HCHO fluxes increases the OH and HO_2 concentrations by $\sim$70% and $\sim$50%, respectively (100 m mixing height).

While the measured diurnal variation in atmospheric H_2O_2 is about a factor of 4 ($\sim$0.4 to $\sim$1.6 ppbv), the gas phase photochemistry alone results in a diurnal change of only 20%, indicating that heterogeneous processes are also taking place. Including a strong heterogeneous deposition due to fog formation and

Figure 3

taking into account the generally lower mixing height at nighttime would increase this amplitude as well as alter the flux - mixing ratio relationship shown in Figure 3 (see section 4.5).

Although the details of halogen activation mechanisms are not completely understood, the role of halogen atoms in Arctic photochemistry is well established [*Rudolph et al.,* 1999; *Boudries and Bottenheim,* 2000]. This role is episodic and is associated with ozone depletion events [*Solberg et al.,* 1996]. There is neither direct or indirect evidence for halogen atom involvement during the time of the Summit observations, nor evidence ruling out such involvement. We have therefore performed a few model runs to estimate the effect that reactions involving chlorine might have on H_2O_2 and HCHO mixing ratios. The oxidation of CH_3Cl and CH_3Br by OH, included in all model runs, does not produce enough active halogen to influence the mixing ratios of other species. We have therefore included a chlorine source to maintain a Cl atom concentration of the order of $10^{10}\,m^{-3}$ [*Rudolph et al.,* 1999]. This increased the H_2O_2 and HCHO mixing ratios by 0.9 and 0.18 ppbv, respectively, due to Cl atom reaction with methane and other hydrocarbons. Without considering the effect of the observed H_2O_2 and HCHO fluxes, a Cl atom concentration similar to that inferred by *Jobson et al.* [1994] increases computed peroxide and formaldehyde concentrations to within about 20% and 13%, respectively, of their observed values. This suggests that halogen photochemistry may, when considered in conjunction with observed H_2O_2 and HCHO fluxes, help resolve discrepancies in the magnitude of observed and computed concentrations. A potential source of Cl atoms may be the proposed HCl volatilization from snow [*Wagnon et al.,* 1999]. However, the reaction of HCl with OH producing Cl atoms appears to be too slow to provide a major Cl source. Due to lack of evidence for halogen involvement at the time of the Summit observations, we have not attempted a best fit of observed H_2O_2 and HCHO fluxes and halogen sources to modeled concentrations.

4.3. Firn Air

Firn air measurements 5 cm below the snow surface on June 20 revealed H_2O_2 mixing ratios up to 3.5 times atmospheric concentrations, consistent with H_2O_2 release by the snow grains (Table 1). Note that due to the porous nature of the firn, the firn air measured is a mixture of atmospheric and firn air, and mixing ratios represent lower limits for actual values. Modeled firn air concentrations for corresponding times and depths agree with the measurements with differences less than 20% (Table 1). The latter are explainable by uncertainties in the surface snow concentrations after June 18 (no minipit data) and the uncertainties in the modeled snow temperatures in the top layers. Previous firn air measurements deeper down (below 25 cm) revealed values near or below the atmospheric level [*Bales et al.,* 1995a], which is consistent with lower temperatures and lower H_2O_2 concentrations in those firn layers.

4.4. Snow

H_2O_2 concentrations in the surface snow layers generally decreased with depth and replicate samples from the top layer had relatively low variability (Figure 1e). The drifting snow samples (open circles in Figure 1e), which could also contain fresh snow (see methods), showed concentrations up to 1200 parts per billion by weight (ppbw). Up to and including June 16 snow falls were light and not expected to contribute significantly to the surface snow samples. Fresh snow collected the night of June 17 had concentrations between 415 ppbw and 720 ppbw (stars in Figure 1e). Pit measurements revealed the typical seasonal H_2O_2 signal with high values (∼350 ppbw) in summer layers and low values (∼50 ppbw) in winter layers [*Hutterli et al.,* 1999]. All previous summer peak values in the pit profile were below 400 ppbw.

The strong H_2O_2 decrease in the top 2-cm snow layer (Figure 1e) from June 6 to June 16 corresponds to a mean H_2O_2 flux of $3.3\times10^{13}\,m^{-2}\,s^{-1}$ (snow density $350\,kg\,m^{-3}$, decrease of $23\,ppbw\,d^{-1}$). Simulating the uptake and release of H_2O_2 from the snow with the transfer model as environmental conditions change shows that deeper layers also significantly contributed to the net flux. Both air-snow partitioning and rates of uptake and release are related to grain size. While the latter was not measured, using effective grain radii within published values led to a good agreement between the modeled and measured evolution of the near-surface snow profiles (Figure 4). As near-surface snow grain radii are significantly smaller than at depth [*Waddington et al.,* 1996], the top 0.5 cm snow layer was set to a constant 100 μm, while only the values for the deeper layers were varied. Table 2 summarizes the model results. The minipit data (and the corresponding flux estimate) were best reproduced with effective snow grain radii of about 120 μm (Figure 4) for those layers. In this case, with a modeled flux from the top 2 cm snow

Figure 4

Table 2

layer of $3.2\times10^{13}\,m^{-2}\,s^{-1}$ ($3.3\times10^{13}\,m^{-2}\,s^{-1}$ from the minipit measurements), the modeled total net flux from the snowpack was $4.6\times10^{13}\,m^{-2}\,s^{-1}$. This is in excellent agreement with the independently determined average flux based on the gradient measurements ($4.9\times10^{13}\,m^{-2}\,s^{-1}$), thus confirming physical uptake/release as the dominant process. Note that if the net H_2O_2 flux revealed by the gradient measurements was due to heterogeneous photochemical H_2O_2 production in the snowpack, the snow would tend to take up the produced H_2O_2 [*Conklin et al.,* 1993], leading to an increase rather than the observed decrease of H_2O_2 concentrations in the snow. Because the combination of grain size and H_2O_2 diffusivity in ice determines the release of H_2O_2, instead of adjusting the grain size, the temperature dependance of the diffusivity could be varied within its uncertainty range as well (changing the diffusivities within a factor of 2-3). While this alters the value of the optimal effective grain size, it does not significantly affect the resulting fluxes. By adjusting the grain size, the model is tuned to account implicitly also for other temperature-dependent processes, such as evaporation and condensation of water vapor on ice crystal surfaces, which are expected to affect the H_2O_2 uptake and release through cocondensation and coevaporation [*Sigg et al.,* 1992].

The very strong depletion of the surface snow layers between June 16 and June 18 ($177\,ppbw\,d^{-1}$, corresponding to $2.5\times10^{14}\,m^{-2}\,s^{-1}$) are coincident with high temperatures, very high wind speeds, and elevated atmospheric H_2O_2 mixing ratios, consistent with the temperature-dependent uptake/release hypothesis. Increased sublimation rates expected during such conditions would accelerate the H_2O_2 depletion in the snow. Part of the depletion could also be due to a removal of the top snow layer by the wind and/or its mixing with lower concentration drifting snow. However, this alone would not explain the elevated atmospheric mixing ratios. The concurrence of high H_2O_2 concentrations in fresh and drifting snow samples with high atmospheric values further stress the close link between the two.

Deposition of fresh snow could explain the higher surface snow layer concentration after June 18. The early June increase in surface snow H_2O_2 concentration occurred during an exceptional fog event lasting from June 4, 22:30 Local Standard Time (LST; UT - 2 hours) through June 6, 04:00 LST that deposited $\sim$1 cm of surface hoar. The concentration was in the range of previous fog and hoar measurements (680 up to 2550 ppbw), agreed with that based on cocondensation theory [*Sigg et al.,* 1992] and was supersaturated with respect to air-snow equilibrium [*Conklin et al.,* 1993; *McConnell et al.,* 1997].

Thus fresh snow and extensive fog deposition can result in higher concentrations in surface snow and can temporarily mask the long-term H_2O_2 release. The previously reported net H_2O_2 increase in surface snow over a 17-day-long period without fresh snow deposition [*Bales et al.,* 1995b] does not exclude a release. Over the 17-day period, the surface snow concentration revealed H_2O_2 enrichments in the course of a day consistent with the reported fog deposition, followed by gradual decreases over several days as expected from the uptake/release hypothesis.

4.5. Fog

While the transfer model reveals a temporary H_2O_2 uptake by the cold surface snow on many nights, it is plausible that fog deposition dominates nighttime H_2O_2 depletion from air [*Sigg et al.,* 1992; *Bergin et al.,* 1996]. Heterogeneous deposition due to fog formation, which occurred on virtually every night during the first 12 days of the measurements, and the lower mixing heights at night can explain the discrepancy. This is supported by sporadic observations in the field linking the fast H_2O_2 depletion in the air to the formation of radiative fog. In fact, modeled fog formation and deposition suggested a complete depletion of atmospheric H_2O_2 in the air [*Bergin et al.,* 1996] which is in contradiction to our measurements. However, these measurements may represent H_2O_2 in the air and in fog droplets, as no attempt was made to prevent the latter from entering the system. This indicates that during fog events much of the H_2O_2 may be present in the fog droplets.

Nighttime ground fog strongly influences atmospheric H_2O_2 mixing ratios and also impacts the surface snow concentrations. However, apart from the exceptional fog event from June 4 to June 6 discussed in the previous section, the impact of fog deposition on surface snow appeared to be small. Specifically, during the June 6 to 16 period, fog observations, minipit measurements and visual surface snow inspection do not indicate a significant impact of fog deposition on the surface snow H_2O_2 concentrations. One exception might have been the fog event on June 9. After this event, fresh surface frost and an increase in surface snow concentrations exceeding the general spatial variability was seen. However, accounting for the potential additional H_2O_2 release following fog

deposition increased the H_2O_2 flux estimate based on the minipit measurements by less than 10% and was therefore neglected.

Fog droplets that are in or close to Henry's equilibrium with the air become highly oversaturated when they freeze. Though rime and surface hoar start releasing H_2O_2 right after formation, the H_2O_2 escaping into the atmosphere is immediately scavenged again by depositing fog droplets and redeposited until the fog droplet flux to the surface stabilizes or decreases, which occurs before air temperatures rise [*Bergin et al.,* 1996]. This change in water flux would thus explain why the snowpack started to release H_2O_2 around midnight, hours before the temperature began to rise (Figure 2). *Sigg et al.*'s [1992] suggestion that the reevaporation of freshly formed hoar was responsible for the rise of the H_2O_2 mixing ratios only holds after the temperature starts to rise. *Bergin et al.* [1996] attributed the morning increase of H_2O_2 in the air to downmixing of higher concentration air from above the fog. However, the atmosphere generally remained stable until around 07:00 LST (Figure 2e) and downmixing is incompatible with the direction of the measured gradients.

5. Conclusions

While heterogeneous photochemical H_2O_2 production in snow can not be excluded, our results show that physical processes are necessary and sufficient to explain the H_2O_2 measurements in snow and air. They show that polar snow and most likely clean, dry snow in general acts as a reservoir for atmospheric H_2O_2. High concentrations of H_2O_2 are incorporated into snow when it forms (cocondensation, riming). Once on the ground, the H_2O_2 both degasses from the snow as it approaches equilibrium and cycles between the atmosphere and surface snow in response to the diurnal temperature cycle and the deposition/evaporation of water. This (re)cycling increases the average H_2O_2 concentration by a factor of 7 above what it would be without a snowpack source, thus contributing ~85% of the H_2O_2 in the planetary boundary layer during the warm part of the day at Summit in summer 1996. The cycling also causes a significant depletion from the air at night. Much of the nighttime atmospheric H_2O_2 may be present in fog droplets, where it represents a strong oxidant that may significantly enhance sulfate deposition [*Bergin et al.,* 1996]. Slow H_2O_2 degassing from snow accounted for the decrease in surface snow concentrations, although modeling studies indicate that the snow is generally buried before reaching equilibrium with the atmosphere at Summit.

This release does not only significantly increase the oxidizing capacity in the planetary boundary layer but also in the firn air in the top snow layers, possibly affecting heterogeneous (photo-)chemistry at the snow crystal surfaces. The temperature dependence of the H_2O_2 release suggests a strong seasonal variation of the fluxes with generally higher values during the warmer months modulated by the timing and concentration of snow accumulation. It further implies that volatile contaminants physically removed from the atmosphere and immobilized in the snow during winter could be partially reemitted in spring while snow temperatures rise. In order to understand the photochemistry in the polar boundary layer and to quantitatively interpret chemical ice core records of volatile species, highly nonlinear physical processes as well as heterogeneous photochemistry in the snowpack must be considered and their impact on regional to global scale assessed.

Acknowledgments. Field measurements were made under the European project EV5V-0412 Transfer of Aerosols and Gases to Greenland Snow and Ice. C.R. Stearns, University of Wisconsin-Madison, funded by NSF, provided the AWS-data (http://uwamrc.ssec.wisc.edu/aws/awsproj.html) and J.E. Dibb provided fresh snow observations. Carbon monoxide and ozone measurements were made available by the National Oceanic and Atmospheric Administration (NOAA), Climate Monitoring and Diagnostics Laboratory (CMDL), Carbon Cycle Group. The Swiss and U.S. National Science Foundations provided financial support. H.W.J. thanks the Deutsche Forschungsgemeinschaft (DFG) for a stipend. We thank C.M. Brown-Mitic and R. Röthlisberger for valuable discussions.

References

Anklin, M., and R. C. Bales, Recent increase in H_2O_2 concentration at Summit, Greenland, *J. Geophys. Res., 102*, 19,099–19,104, 1997.

Atkinson, R., D. L. Baulch, R. F. Hampson Jr., J. A. Kerr, and J. Troe, Evaluated kinetic and photochemical data for atmospheric chemistry, *J. Phys. Chem. Ref. Data, 21,* suppl. IV, 1125–1568, 1992.

Bales, R. C., M. V. Losleben, J. R. McConnell, K. Fuhrer, and A. Neftel, H_2O_2 in snow, air and open pore space in firn at Summit, Greenland, *Geophys. Res. Lett., 22,* 1261–1264, 1995a.

Bales, R. C., J. R. McConnell, M. V. Losleben, M. H. Conklin, K. Fuhrer, A. Neftel, J. E. Dibb, J. D. W. Kahl, and C. R. Stearns, The diel variations of H_2O_2 in Greenland: A discussion of the cause and effect relationship, *J. Geophys. Res., 100*, 18,661–18,668, 1995b.

Bergin, M. H., S. N. Pandis, C. I. Davidson, J.-L. Jaffrezo, J. E. Dibb, A. G. Russell, and H. D. Kuhns, Modeling of the processing and removal of trace gas and aerosol species by Arctic radiation fogs and comparison with measurements, *J. Geophys. Res., 101*, 14,465–14,478, 1996.

Boudries, H., and J. W. Bottenheim, Cl and Br atom concentrations during a surface boundary layer ozone depletion event in the Canadian High Arctic, *Geophys. Res. Lett., 27*, 517–520, 2000.

Colbeck, S. C., Snow-crystal growth with varying surface temperatures and radiation penetration, *J. Glaciol., 35*, 23–29, 1989.

Conklin, M. H., A. Sigg, A. Neftel, and R. C. Bales, Atmosphere-snow transfer function for H_2O_2: Microphysical considerations, *J. Geophys. Res., 98*, 18,367–18,376, 1993.

Couch, T. L., A. L. Sumner, T. M. Dassau, P. B. Shepson, and R. E. Honrath, An investigation of the interaction of carbonyl compounds with the snowpack, *Geophys. Res. Lett., 27*, 2241–2244, 2000.

DeMore, W. B., S. P. Sander, D. M. Golden, R. F. Hampson, M. J. Kurylo, C. J. Howard, A. R. Ravishankara, C. E. Kolb, and M. J. Molina, Chemical kinetics and photochemical data for use in stratospheric modeling, *JPL Publ., 97-12*, 1997.

Fuhrer, K., M. Hutterli, and J. R. McConnell, Overview of recent field experiments for the study of the air-snow transfer of H_2O_2 and HCHO, in *Chemical Exchange Between the Atmosphere and Polar Snow*, *NATO ASI Ser. I, Vol. 43,* pp. 307-318, Springer-Verlag, New York, 1996.

GLOBALVIEW-CH4, *Cooperative Atmospheric Data Integration Project - Methane* [CD-ROM], NOAA Clim. Monit. and Diagnostics Lab., Boulder, Colo., 1999.

Graedel, T. E., and W. C. Keene, Tropospheric budget of reactive chlorine, *Global Biogeochem. Cycles, 9*, 47–77, 1995.

Högström, U., Non-dimensional wind and temperature profiles in the atmospheric surface layer: A re-evaluation, *Boundary Layer Meteorol., 42*, 55–78, 1988.

Honrath, R. E., S. Guo, M. C. Peterson, M. P. Dziobak, J. E. Dibb, and M. A. Arsenault, Photochemical production of gas phase NO_x from ice crystal NO_3^-, *J. Geophys. Res., 105*, 24,183–24,190, 2000.

Hutterli, M. A., Luft-Firn Transferstudien von HCHO und H_2O_2 zur Interpretation von Eisbohrkerndaten, Ph.D. thesis, Phys. Inst., Univ. of Bern, Bern, Switzerland, 1999.

Hutterli, M. A., R. Röthlisberger, and R. C. Bales, Atmosphere-to-snow-to-firn transfer studies of HCHO at Summit, Greenland, *Geophys. Res. Lett., 26*, 1691–1694, 1999.

Jobson, B. T., H. Niki, Y. Yokouchi, J. Bottenheim, F. Hopper, and R. Leaitch, Measurements of C_2-C_6 hydrocarbons during the Polar Sunrise 1992 Experiment: Evidence for Cl and Br atom chemistry, *J. Geophys. Res., 99*, 25,355–25,368, 1994.

Jones, A. E., R. Weller, E. W. Wolff, and H.-W. Jacobi, Speciation and rate of photochemical NO and NO_2 production in Antarctic snow, *Geophys. Res. Lett., 27*, 345–348, 2000.

King, J. C., and P. S. Anderson, Heat and water vapor fluxes and scalar roughness lengths over an Antarctic ice shelf, *Boundary Layer Meteorol., 69*, 101–121, 1994.

King, J. C., P. S. Anderson, M. C. Smith, and S. D. Mobbs, The surface energy and mass balance at Halley, Antarctica during winter, *J. Geophys. Res., 101*, 19,119–19,128, 1996.

Madronich, S., Photodissociation in the atmosphere, 1. Actinic flux and the effect of ground radiation and clouds, *J. Geophys. Res., 92*, 9740–9752, 1987.

McConnell, J. R., J. R. Winterle, R. C. Bales, A. M. Thompson, and R. W. Stewart, Physically based inversion of surface snow concentrations of H_2O_2 to atmospheric concentrations at South Pole, *Geophys. Res. Lett., 24*, 441–444, 1997.

McConnell, J. R., R. C. Bales, R. W. Stewart, A. M. Thompson, and M. R. Albert, Physically based modeling of atmosphere-to-snow-to-firn transfer of H_2O_2 at South Pole, *J. Geophys. Res., 103*, 10,561–10,570, 1998.

Neftel, A., R. C. Bales, and D. J. Jacob, H_2O_2 and HCHO in polar snow and their relation to atmospheric chemistry, in *Ice Core Studies of Global Biogeochemical Cycles, NATO ASI Ser I, vol. 30*, edited by R. J. Delmas, pp. 249–264, Springer-Verlag, New York, 1995.

Poisson, N., M. Kanakidou, and P. J. Crutzen, Impact of non-methane hydrocarbons on tropospheric chemistry and the oxidzing power of the global troposphere: 3-dimensional modelling results, *J. Atmos. Chem., 36*, 157–230, 2000.

Röthlisberger, R., M. Bigler, M. A. Hutterli, S. Sommer, B. Stauffer, H. G. Junghans, and D. Wagenbach, Technique for continuous high-resolution analyses of trace substances in firn and ice cores, *Environ. Sci. Technol., 34*, 338–342, 2000.

Rudolph, J., R. F. Ban, A. Thompson, K. Anlauf, and J. Bottenheim, Halogen atom concentrations in the Arctic troposphere derived from hydrocarbon measurements: Impact on the budget of formaldehyde, *Geophys. Res. Lett., 26*, 2941–2944, 1999.

Schwander, J., T. Sowers, J.-M. Barnola, T. Blunier, A. Fuchs, and B. Malaiz, Age scale of the air in the Summit ice: Implications for glacial-interglacial temperature change, *J. Geophys. Res., 102*, 19,483–19,493, 1997.

Seinfeld, J. H., and S. N. Pandis, *Atmospheric Chemistry and Physics*, John Wiley, New York, 1998.

Sigg, A., and A. Neftel, Evidence for a 50% increase in H_2O_2 over the past 200 years from a Greenland ice core, *Nature, 351*, 557–559, 1991.

Sigg, A., T. Staffelbach, and A. Neftel, Gas phase measurements of hydrogen peroxide in Greenland and their meaning for the interpretation of H_2O_2 records in ice cores, *J. Atmos. Chem., 14*, 223–232, 1992.

Solberg, S., N. Schmidbauer, A. Semb, F. Stordal, and O. Hov, Boundary-layer ozone depletion as seen in the Norwegian Arctic in spring, *J. Atmos. Chem., 23*, 301–332, 1996.

Stewart, R. W., Multiple steady states in atmospheric chemistry, *J. Geophys. Res., 98*, 20,601–20,611, 1993.

Stewart, R. W., Dynamics of the low to high NO_x transition in a simplified tropospheric photochemical model, *J. Geophys. Res., 100*, 8929–8943, 1995.

Stewart, R. W., and A. M. Thompson, Kinetic data imprecisions in photochemical rate calculations: Means, medians, and temperature dependence, *J. Geophys. Res., 101*, 20,953–20,964, 1996.

Stewart, R. W., S. Hameed, and G. Matloff, A model study of the effects of intermittent loss on odd nitrogen concentrations in the lower troposphere, *J. Geophys. Res., 88*, 10,697–10,707, 1983.

Sumner, A.-L., and P. B. Shepson, Snowpack production of formaldehyde and its effect on the Arctic troposphere, *Nature, 398*, 230–233, 1999.

Thompson, A. M., The oxidizing capacity of the Earth's atmosphere: Probable past and future changes, *Science, 256*, 1157–1168, 1992.

Waddington, E. D., J. Cunningham, and S. L. Harder, The effects of snow ventilation on chemical concentrations, in *Chemical Exchange Between the Atmosphere and Polar Snow*, *NATO ASI Ser. I, vol. 43,* pp. 403–451, Springer-Verlag, New York, 1996.

Wagnon, P., R. J. Delmas, and M. Legrand, Loss of volatile acid species from upper firn layers at Vostok, Antarctica, *J. Geophys. Res., 104*, 3423–3431, 1999.

Yokouchi, Y., L. A. Barrie, D. Toom-Sauntry, Y. Nojiri, Y. Fujinuma, Y. Inuzuka, H. J. Li, H. Akimoto, and S. Aoki, Latitudinal distribution of atmospheric methyl bromide: Measurements and modeling, *Geophys. Res. Lett., 27*, 697–700, 2000.

R. C. Bales, M. A. Hutterli, and H.-W. Jacobi, Department of Hydrology and Water Resources, University of Arizona, Tucson, AZ 85721. (roger@hwr.arizona.edu; manuel@hwr.arizona.edu; hwj@hwr.arizona.edu)

J. R. McConnell, Desert Research Institute, Water Resources Center, 2215 Raggio Parkway, Reno, NV 89512. (jmcconn@dri.edu)

R. W. Stewart, NASA GSFC, Code 916, Greenbelt, MD 20771. (stewart@oasis.gsfc.nasa.gov)

September 25, 2000; revised January 31, 2001; accepted February 3, 2001.

[1]Department of Hydrology and Water Resources, University of Arizona, Tucson, Arizona.

[2]Desert Research Institute, Reno, Nevada.

[3]NASA Goddard Space Flight Center, Greenbelt, Maryland.

This preprint was prepared with AGU's LaTeX macros v4. File H2O2˙jgr˙final˙sent˙2col formatted April 21, 2001.

Figure 1. Results of H_2O_2 and meteorological measurements at Summit. Diamonds below the time axis indicate reported fog, and stars indicate snow precipitation. (a) Atmospheric H_2O_2 mixing ratios. (b) Corresponding H_2O_2 gradients between 3.5 and 0.06 m. Open circles are measurements at fixed height of 3.5 m, which do not represent gradients, but rather the variability of the H_2O_2 mixing ratios in the air on timescales of the gradient measurements ($\sim$20 min). (c) Air temperature (3 m). (d) Wind speed (3 m). (e) H_2O_2 concentrations in the top snow layers in parts per billion by weight (ppbw). Drifting snow is a mixture of fresh and wind-blown snow.

Figure 2. Average diurnal cycles in Local Standard Time (LST) for the period from June 4 to June 16, 1996 (hour of day averages are based on 10-min data). (a) Atmospheric H_2O_2 mixing ratios. (b) Corresponding H_2O_2 gradients between 3.5 and 0.06 m with standard deviation of the mean. (c) Calculated H_2O_2 fluxes from the snowpack. (d) Air temperature. (e) Air temperature gradient.

Figure 3. Modeled atmospheric H_2O_2 and HCHO mixing ratios as a function of H_2O_2 fluxes for two mixing heights. Solid lines indicate results calculated without a HCHO flux, and dotted lines indicate results calculated with a HCHO flux of $1\times10^{13}\,m^{-2}\,s^{-1}$.

Figure 4. Measured and corresponding modeled (solid lines) H_2O_2 concentrations in the surface snow using a grain size of 120 μm (100 μm for the top layer).

Table 1. Comparison of the June 20 H_2O_2 Firn Air Measurements With Model Results[a]

Time, LST	Air Temperature, °C	C_a, ppbv	C_{fa}, ppbv	C_{fa}^{mod}, ppbv
1000	-12	0.60	2.1	1.7
1600	-11	0.76	1.8	1.9
2400	-20	0.62	1.0	0.9

[a] C_a, atmospheric H_2O_2 mixing ratio; C_{fa}, firn air H_2O_2 mixing ratio; C_{fa}^{mod}, modeled firn air H_2O_2 mixing ratio, 0-2.5 cm average.

Table 2. Modeled Mean H_2O_2 Fluxes From the Snowpack Between June 6 and 16

Grain Size,[a] μm	F_{2cm},[b] $10^{13}\,m^{-2}\,s^{-1}$	F_{total},[c] $10^{13}\,m^{-2}\,s^{-1}$
100	3.52	5.68
120	3.24	4.61
150	2.98	3.70
180	2.80	3.19
250	2.56	2.59

[a]Grain size fixed at 100 μm in the top 0.5 cm.

[b]H_2O_2 flux from the top 2 cm snow layer.

[c]Total H_2O_2 flux from the snowpack.

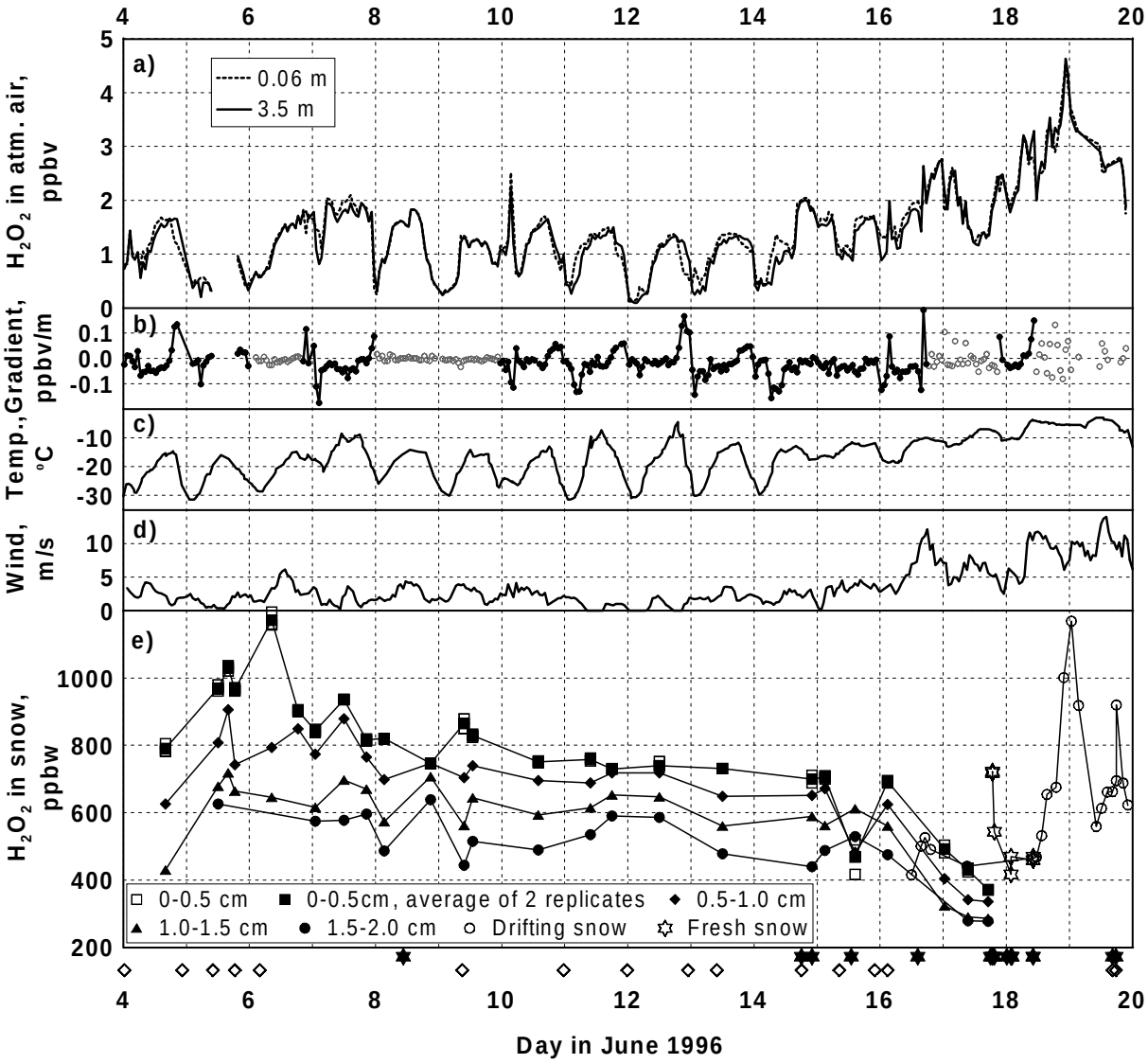
a)
0.06 m
3.5 m
H_2O_2 in atm. air, ppbv
b)
Gradient, ppbv/m
c)
Temp., °C
d)
Wind, m/s
e)
H_2O_2 in snow, ppbw
0-0.5 cm
0-0.5cm, average of 2 replicates
0.5-1.0 cm
1.0-1.5 cm
1.5-2.0 cm
Drifting snow
Fresh snow
Day in June 1996

Figure 1

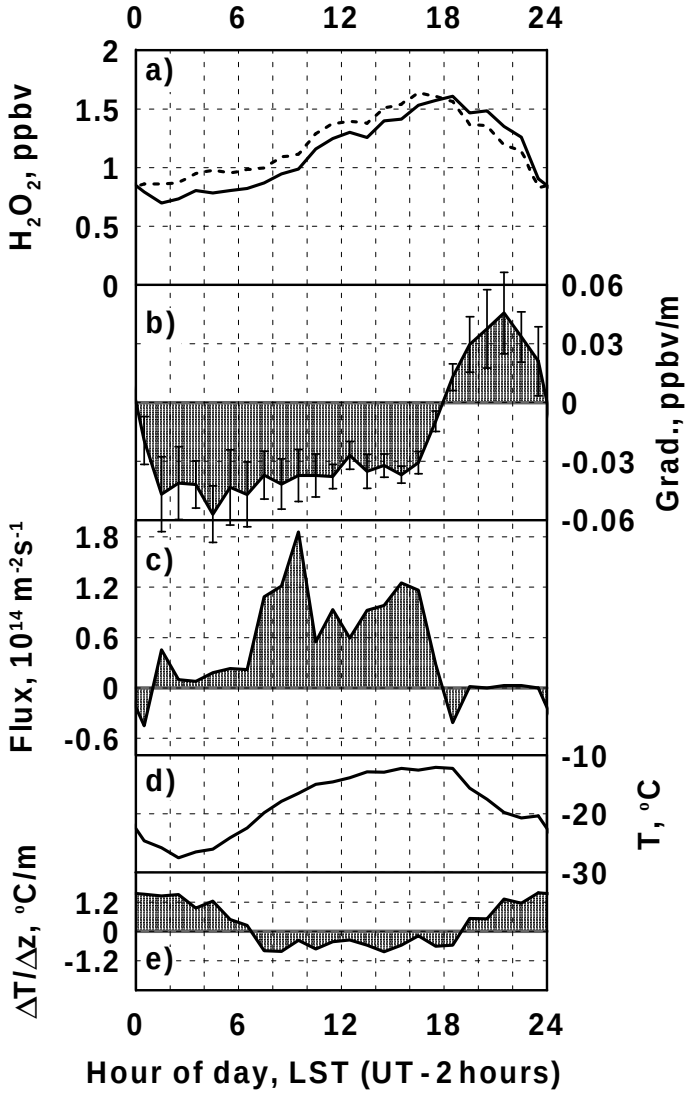
0
6
12
18
24
a)
b)
c)
d)
e)
H_2O_2, ppbv
2
1.5
1
0.5
0
0.06
0.03
0
-0.03
-0.06
Grad., ppbv/m
Flux, 10^{14} $m^{-2}s^{-1}$
1.8
1.2
0.6
0
-0.6
-10
-20
-30
T, °C
$\Delta T/\Delta z$, °C/m
1.2
0
-1.2
Hour of day, LST (UT - 2 hours)

Figure 2

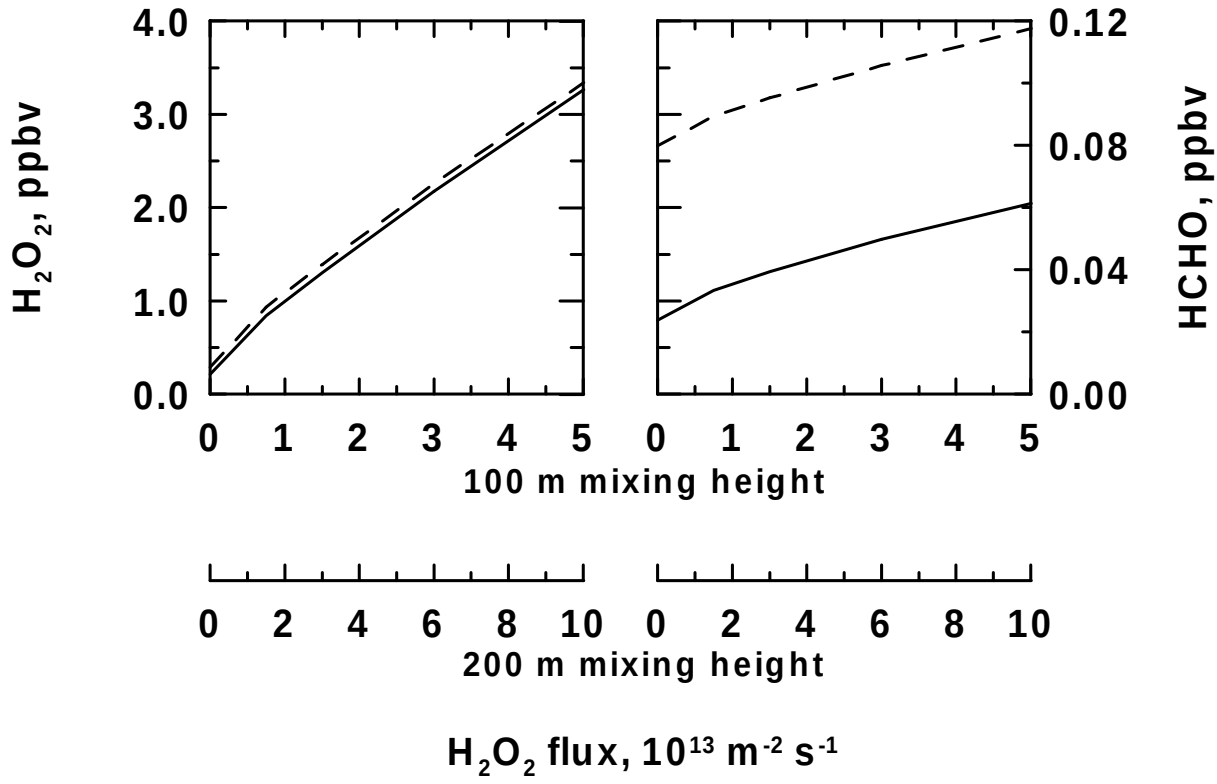
4.0
3.0
2.0
1.0
0.0
H2O2, ppbv
0.12
0.08
0.04
0.00
HCHO, ppbv
0 1 2 3 4 5
0 1 2 3 4 5
100 m mixing height
0 2 4 6 8 10
0 2 4 6 8 10
200 m mixing height
H2O2 flux, 10^13 m^-2 s^-1

Figure 3

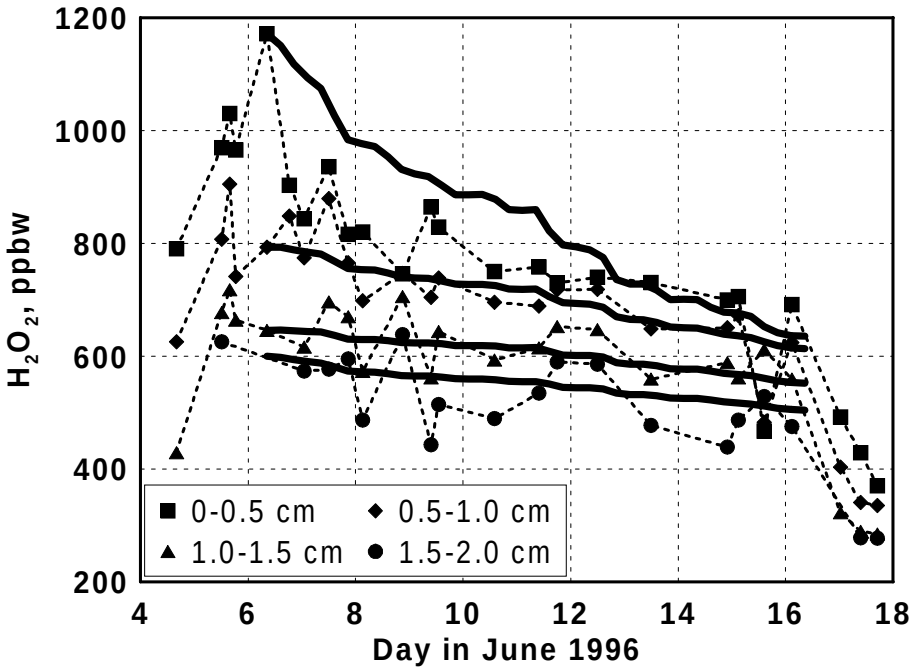
1200
1000
800
600
400
200
H_2O_2, ppbw
4
6
8
10
12
14
16
18
Day in June 1996
0-0.5 cm
0.5-1.0 cm
1.0-1.5 cm
1.5-2.0 cm

Figure 4